J Appl Electrochem (2010) 40:507–513
DOI 10.1007/s10800-009-0022-0

ORIGINAL PAPER

Characterization of copper–silicon nitride composite electrocoatings

Alain Robin · Júlio Cesar Pinheiro de Santana · Antonio Fernando Sartori

Received: 19 May 2009 / Accepted: 25 September 2009 / Published online: 11 October 2009

Abstract Silicon nitride particles were incorporated to electrolytic copper by co-electrodeposition in acidic sulfate bath, aiming the improvement of its mechanical resistance. Smooth deposits containing well-distributed silicon nitride particles were obtained. The current density did not show significant influence on incorporated particle volume fraction, whereas the variation of particle concentration in the bath had a more pronounced effect. The microhardness of the composite layers was higher than that of pure copper deposits obtained under the same conditions and increased with the increase of incorporated particle volume fraction. The microhardness of composites also increased with the increase of current density due to copper matrix grain refining. The composite coatings were slightly more corrosion resistant than pure copper deposits in 3.5% NaCl solutions.

Keywords Electrodeposition · Copper · Silicon nitride · Composite · Characterization · Corrosion

1 Introduction

Electrodeposition is widely used for the production of metallic coatings, such as copper, nickel, tin, chromium, and noble metals electroplates. This is a cheap technique that does not require sophisticated equipments. In order to improve some properties of these metallic coatings (for example, hardness, wear resistance, and corrosion resistance), researches were developed incorporating particles of ceramic, metallic, and polymeric materials to the electrodeposits [1, 2]. The co-electrodeposition consists in electrolyzing a solution containing the metallic salts and the particles in suspension. The main factors that influence the amount of incorporated particles, and consequently the properties of the composite coatings, are the electrolysis parameters (composition of the bath, pH, temperature, cathodic current density, stirring rate) and the parameters related to particles (type, concentration and mean size).

The copper electroplates are widely used in engineering applications due to the high electrical and thermal conductivity of copper, good ductility, and good corrosion resistance. Nevertheless, these coatings show low mechanical and wear resistance. Aiming to modify the properties of electrolytic copper, particles of ceramic materials, Al_2O_3 [3–8], TiO_2 [9, 10], ZrO_2 [11], SiC and MoS_2 [6], metallic materials or intermetallics, Cr [12] and ZrB_2 [13, 14], polymeric materials, poliacrilonitrile (PAN) [15] and also graphite [6], carbon nanofibers [16], and microcapsules containing lubricants [17] were incorporated to copper. The effect of particle incorporation on the copper coating properties was shown to be positive or negative depending on the electrolysis parameters employed and the type and characteristics of particles.

The objective of this study was the production of copper–silicon nitride electrocomposites from acidic sulfate bath and their characterization. The influence of cathodic current density and particle concentration in the bath on the incorporated particle volume fraction and characteristics of the coatings (roughness, microstructure and microhardness) was analysed. The corrosion behavior of the copper–silicon nitride composites was evaluated in NaCl solutions.

A. Robin (✉) · J. C. P. de Santana · A. F. Sartori
Escola de Engenharia de Lorena, Departamento de Engenharia de Materiais, Universidade de São Paulo, CP 116, Lorena, SP 12600-000, Brazil
e-mail: alain@demar.eel.usp.br

2 Experimental procedure

The Cu–Si_3N_4 composite coatings were prepared in acidic sulfate bath (pH = 1.6) containing 150 g L^{-1} $CuSO_4$ and 30 g L^{-1} H_2SO_4 at room temperature. The Si_3N_4 particles were maintained suspended in the solution by magnetic stirring at 400 rpm. The particles employed had a 1.7 μm mean size and their concentration in the bath was 20 and 40 g L^{-1}.

Sheets of AISI 1020 carbon steel with 100 mm × 6 mm × 1 mm dimensions were used as cathodes. These were previously ground to a 600 grit finish, degreased and dried. The cathode was placed at the center of a cylindrical electrolytic copper anode of 40 mm diameter, previously etched in dilute HNO_3. Cathodic current densities of 10, 20, 30, and 40 mA cm^{-2} were applied for 7 h 40 min, 3 h 50 min, 2 h 33 min and 1 h 55 min, respectively, in order to obtain deposits of approximately 100 μm thickness. The effect of current density and particle concentration on the volume fraction of incorporated particles, roughness, texture, and microhardness was investigated.

The morphology of the coatings and the distribution of particles were examined by scanning electron microscopy (SEM; LEO VP-1450) and the crystalline orientation was analysed by X-ray diffractometry (XRD; SIEFERT-DEBYEFLEX 1001, Cu–Kα).

The roughness of the composite coatings was measured using a surface roughness measuring instrument MITUTOYO SJ 201.

The percentage of embedded particles in the deposits was determined from polished cross-section photomicrographs using the Image Tool 2.0 free software. The image analysis operations were performed at 2,000 times magnification on at least 20 fields of view for each coating and the mean volume fraction of incorporated particles was calculated.

The microindentation hardness of the composite coatings was measured on polished cross-sections using a Vickers microhardness tester (MICROMET 2004). A 100 g load was applied for 30 s.

The corrosion behavior of composite coatings was evaluated in naturally aerated 3.5% NaCl solutions at room temperature by potentiodynamic polarization using a typical three-electrodes corrosion cell (working electrode: composite coating; counter electrode: platinum; reference electrode: saturated calomel electrode—SCE). The coatings were immersed for 1 h in the solutions before polarization. Polarization measurements were carried out potentiodynamically at 1 mV s^{-1} sweep rate using an AUTOLAB 30 potentiostat controlled with a personal computer through GPES specific software.

Pure copper electrocoatings were also produced and characterized in the same way as the composite deposits, for comparison purpose.

3 Results and discussion

3.1 Coatings morphology, texture and particle content

The X-ray diffractograms of all the deposits obtained in solutions containing suspended Si_3N_4 particles presented the Si_3N_4 phase characteristic peaks at low angles, proving the incorporation of Si_3N_4 to copper (Fig. 1). All composite coatings obtained under the experimental conditions investigated were well crystallized.

Using the same current density the composites showed a finer surface morphology than the pure copper deposits (Fig. 2). The Si_3N_4 particles inhibited the growth of the copper crystallites and the composite coatings have a copper matrix with smaller crystal sizes comparatively to the pure copper deposits. This was also observed for other copper composites, such as Cu–ZrO_2 [11], Cu–ZrB_2 [13], and Cu–Al_2O_3 [18].

On the other hand, copper grain size in both pure copper and composite coatings was finer when the current density increased, due to a higher crystal nucleation rate (Fig. 2).

Figure 3 shows the surface roughness of pure copper and Cu–Si_3N_4 composite coatings as a function of cathodic current density. All coatings presented low roughness but the composites exhibited the greatest smoothness, with roughness in the 0.6 to 1.5 μm range that decreased with increasing current density. Since both copper and composite coatings are smooth, it is expected that the lower roughness could be related to the lower grain size. This is the case in the present study and this behavior was also reported for other pure metal and composite electrocoatings [19, 20]. The roughness of pure copper deposits tends

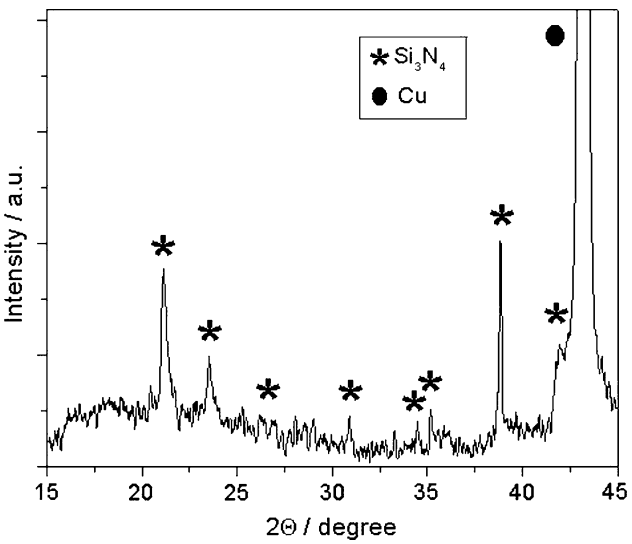

Fig. 1 Typical X-ray pattern at low angles of Cu–Si_3N_4 composite coatings

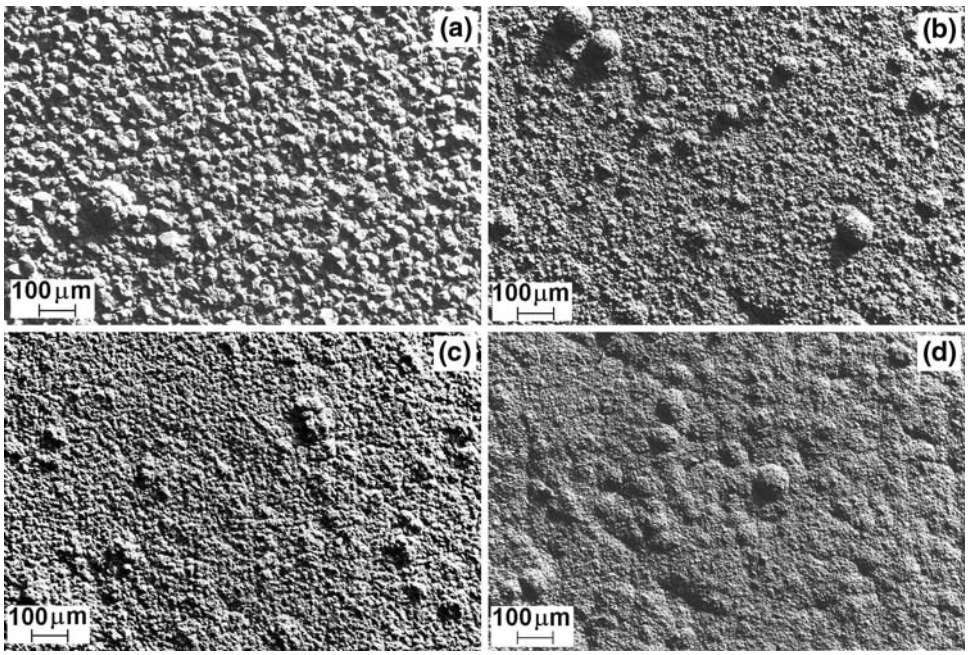

Fig. 2 Surface morphology of pure copper and Cu–Si_3N_4 composite coatings as a function of current density: **a**, **b** pure copper using 20 and 40 mA cm^{-2}, respectively; **c**, **d** composite using 20 and 40 mA cm^{-2}, respectively, and 20 g L^{-1} particle concentration

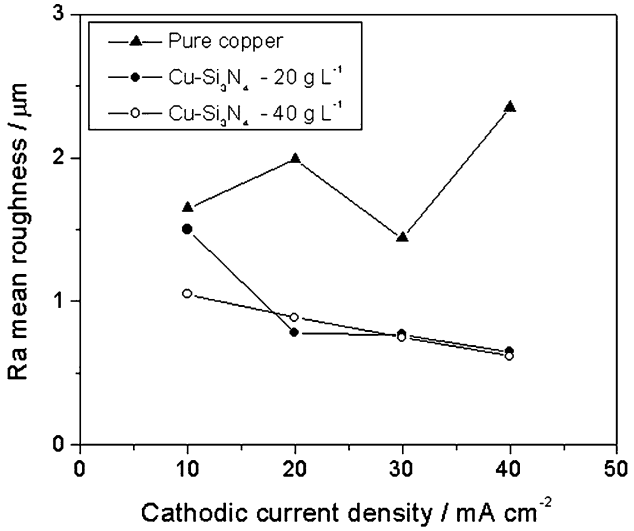

Fig. 3 Ra mean surface roughness of pure copper and Cu–Si_3N_4 composite coatings as a function of cathodic current density

to increase with the increase in current density due to dendritic growth.

The X-ray diffractograms of pure copper and Cu–Si_3N_4 composite are shown in Fig. 4a and b, respectively. The peaks associated to copper phase were indexed using JCPDS data [21]. The peaks relative to Si_3N_4 phase are not visible in Fig. 4b due to their low intensity. The intensity of peaks associated to copper depended on the cathodic current density for both coatings (Fig. 4a, b). The higher intensity of copper diffraction peaks for the composites when compared to pure copper suggests a higher ordering of the copper crystalline planes in composite matrix.

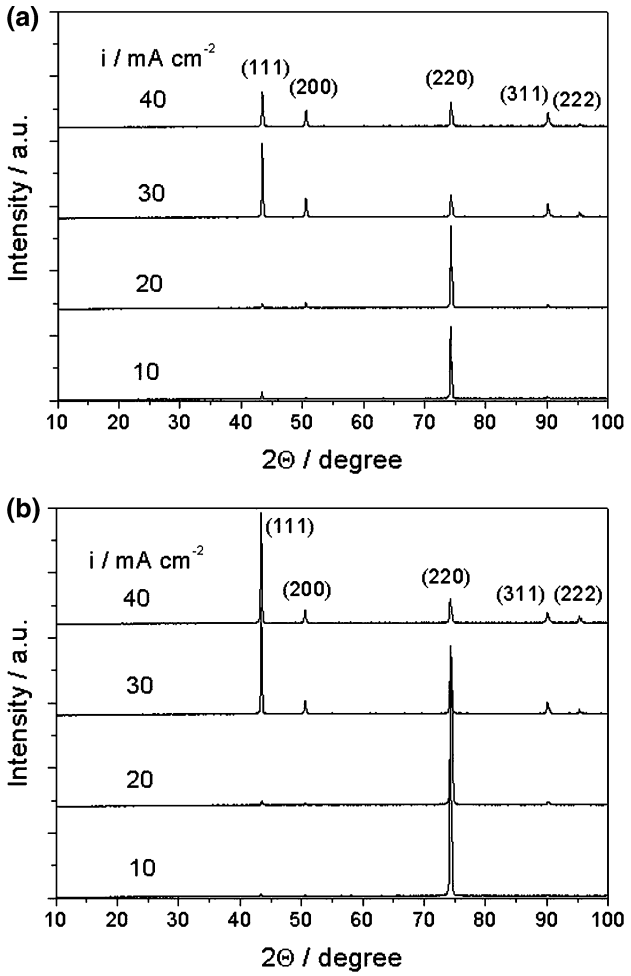

Fig. 4 X-ray diffractograms of **a** pure copper and **b** Cu–Si_3N_4 composite coatings as a function of cathodic current density

It would be expected the opposite effect, i.e., disturbed copper crystallization due to particle incorporation. This point would need more investigation.

The orientation index of the (111), (200), (220), (311) and (222) planes of copper was calculated for each cathodic current density from the Eq. 1:

$$\text{Orientation index} = (I_{hkl}/\Sigma I_{hkl})/(I_{\text{ASTM } hkl}/\Sigma I_{\text{ASTM } hkl}) \quad (1)$$

where I_{hkl} and $I_{\text{ASTM } hkl}$ are the intensities of (hkl) peaks related to copper phase in the coatings and to copper of random orientation [21], respectively.

The copper phase was clearly textured in the [110] direction for both coatings obtained using 10 and 20 mA cm^{-2} current densities (Fig. 5a, b), which means that most copper crystals were oriented with their (220) planes parallel to the surface of the substrate. For both copper and composite coatings this preferential orientation tended to change to a random orientation when current density was increased to 30 and 40 mA cm^{-2}. Thus, the incorporation of Si_3N_4 particles to copper did not affect the orientation of copper grains. In other cases, such as TiO_2 in copper [9] and both WC and Nb in nickel [22, 23], the incorporation of particles to the metallic electrocoating was shown to change the orientation of the matrix crystals.

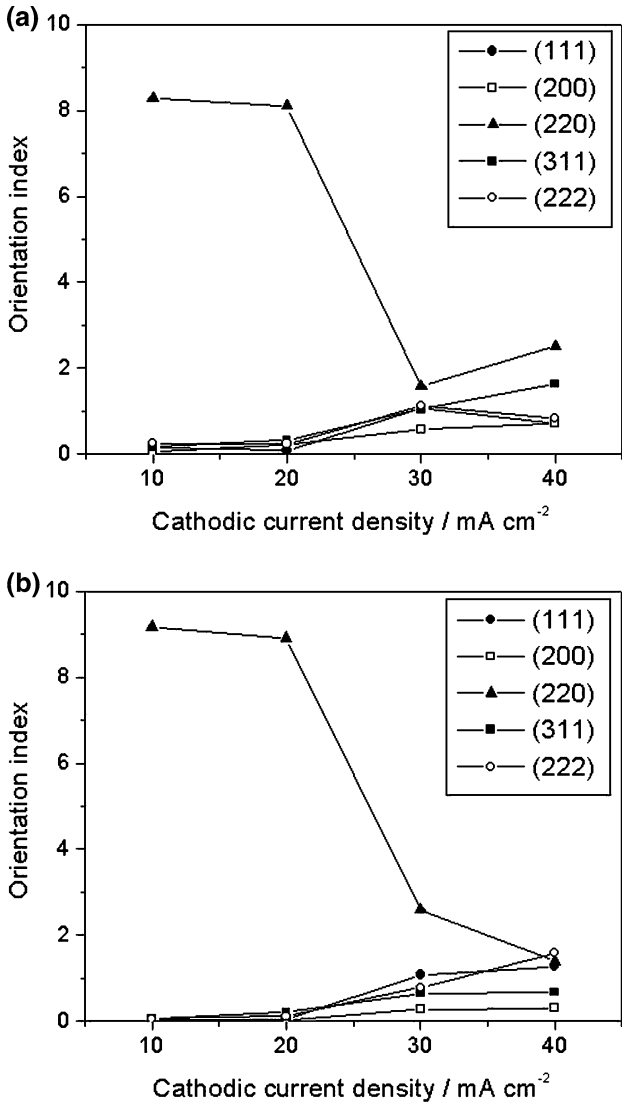

Fig. 5 Orientation index of the (111), (200), (220), (311), and (222) planes of copper phase in **a** pure copper and **b** Cu–Si_3N_4 composite coatings as a function of cathodic current density

Figure 6 shows a typical SEM micrograph of the cross-section of composite coatings. The Si_3N_4 particles appear as dark spots in the lighter copper matrix. The distribution of the Si_3N_4 particles was homogeneous for all composite coatings but the incorporated particle volume fraction was dependent on experimental conditions. The incorporated particle volume fraction measured by image analysis of Fig. 6 was 7.3%.

The influence of cathodic current density and Si_3N_4 particle concentration in the bath on the incorporated particle volume fraction in composite coatings was shown in Fig. 7. The incorporated particle fraction was not influenced by the current density. In the other hand, the increase of particle concentration in the bath from 20 to 40 g L^{-1} decreased the incorporated particle volume fraction.

The comparison of the effect of current density and particle concentration on the incorporated Si_3N_4 particle volume fraction with published results is a hard task since it was verified that the evolution of the amount of incorporated particles to copper is highly dependent on the electrolysis conditions (current density and stirring rate), and type, size, and concentration of particles. For example, Zhu [24] observed an increase in SiC particle content when the current density increased from 20 to 50 mA cm^{-2} but a decrease for densities higher than 50 mA cm^{-2}. In the other hand, Hayashi [5] showed that the incorporated

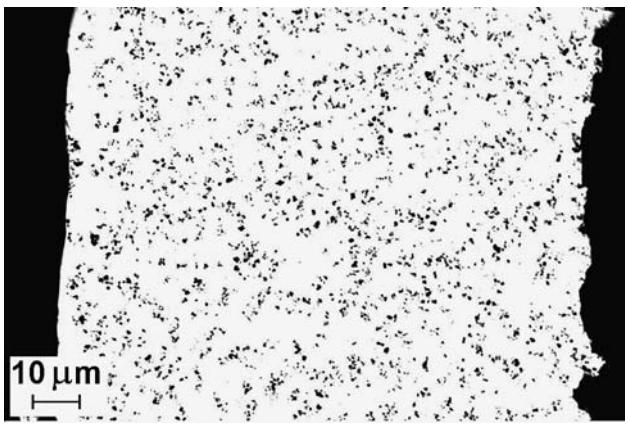

Fig. 6 SEM micrograph (backscattered mode) of cross-section of a Cu–Si_3N_4 composite coating obtained in a bath containing 20 g L^{-1} Si_3N_4 particles using 20 mA cm^{-2} current density

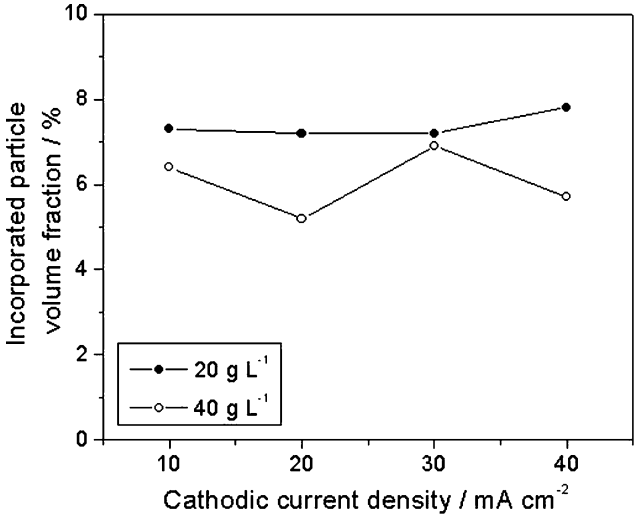

Fig. 7 Incorporated particle volume fraction in Cu–Si_3N_4 composite coatings as a function of cathodic current density and particle concentration in the bath

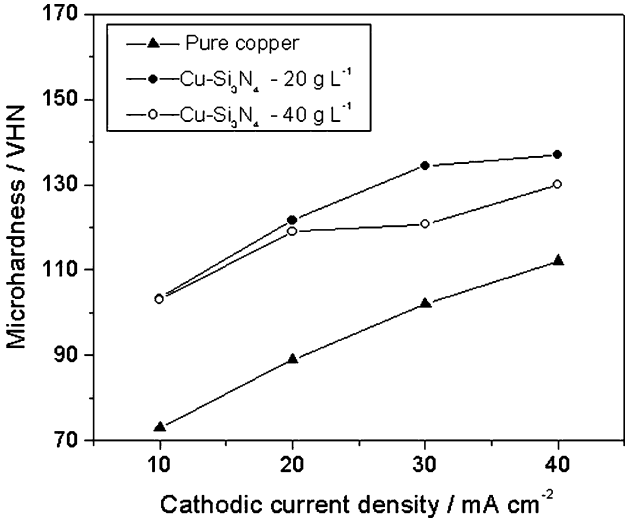

Fig. 8 Microhardness of pure copper and Cu–Si_3N_4 composite coatings as a function of cathodic current density

Al_2O_3 particle fraction diminished when the current density increased from 10 to 70 mA cm^{-2}. The relative independence of the current density on the incorporated particle fraction under our experimental conditions could be related to the diffusion control of the metallic ions deposition.

In relation to particle concentration effect, Zhu [24] showed an increase of incorporated SiC particle fraction when the particle concentration increased from 15 to 35 g L^{-1} but a decrease between 35 and 45 g L^{-1}. Differently, Stankovic and Gojo [6] evidenced an increase of both Al_2O_3 and SiC particle contents when their concentration in the bath increased from 20 to 125 g L^{-1}. In our case the decrease of the incorporated particle volume fraction with increasing concentration of particles from 20 to 40 g L^{-1} could be due to collision factor. The chance of collisions between particles increases with increasing particle concentration, which could lead to the decrease of the incorporated particle volume fraction.

3.2 Microhardness

The microhardness of Cu–Si_3N_4 composite and pure copper coatings increases with increasing cathodic current density and the evolutions of microhardness are very similar for both materials (Fig. 8). Nevertheless, the microhardness of the composites was higher than that of pure copper.

The increase in microhardness of pure copper electrodeposits with increasing current density has been attributed to copper grain refining [25] and this effect of current density was verified comparing Fig. 2a, b. Since the incorporated particle volume fraction in composites was shown not to depend significantly on cathodic current density (Fig. 7), the increase in composite microhardness with the increase of current density was mainly due to the reduction of copper matrix grain size, as observed comparing Fig. 2c, d.

The microhardness versus incorporated particle volume fraction for the composites obtained under the investigated experimental conditions is presented in Fig. 9. For a given current density a clear tendency of increasing in microhardness with the increase of incorporated Si_3N_4 particle content is observed. The higher microhardness of copper-particle composite coatings when compared to that of pure copper was also observed for the incorporation of other types of particles to copper, such as SiC [6, 24], Al_2O_3 [6, 7], and ZrB_2 [14].

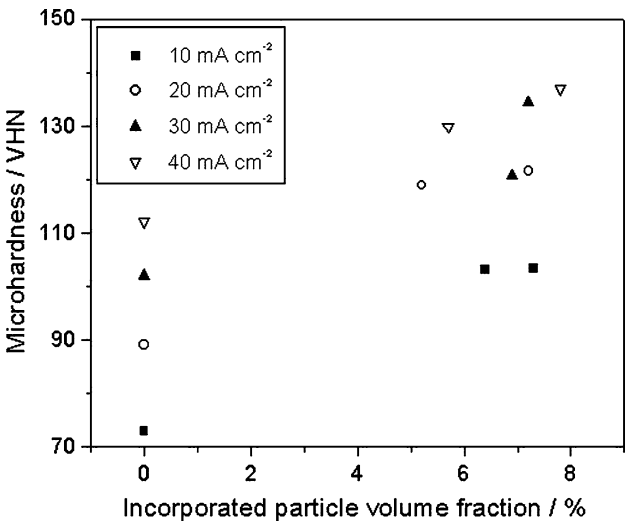

Fig. 9 Microhardness of Cu–Si_3N_4 composites as a function of incorporated particle volume fraction and cathodic current density

The increase in microhardness with Si_3N_4 particle incorporation can be explained by two reasons: (i) dispersion-strengthening and (ii) grain refining. Dispersion-strengthening is associated to the incorporation of fine particles and volume fraction lower than 15% [24] which corresponds to our conditions (Si_3N_4 particle size lower than 2 μm and 7.8% highest incorporated particle volume fraction). In this case, the matrix carries the load and the small particles hinder dislocation motion. Since a reduction of the copper matrix grain size with Si_3N_4 particle incorporation was also observed for a given deposition current density (Fig. 2), grain refining can also explain the higher hardness of the composites.

Particle-strengthening was also proposed to justify hardening of composite coatings [26]. In this case, the load is carried by both the matrix and the particles and strengthening is achieved because the particles restrain the matrix deformation. This mechanism is generally related to the incorporation of hard particles with volume fraction above 20%, which cannot be applied to our case since the highest incorporated Si_3N_4 particle volume fraction was 7.8%.

3.3 Corrosion behavior

The corrosion potentials of pure copper and composite electrocoatings (obtained using 10 and 30 mA cm^{-2} deposition current density) measured after 1 h immersion in 3.5% NaCl solution are the same (Table 1) and are close to the value measured for wrought copper in the same solution, i.e., −0.248 V/SCE [27]. The shapes of the polarization curves of both pure copper and composite coatings (Fig. 10) are also very similar which shows that the anodic and cathodic reactions occurring on both surfaces are identical. The corrosion current densities of pure copper coatings measured using Tafel extrapolation method are also close to the value obtained for wrought copper in the same solution, i.e., 11.9 μA cm^{-2} [27], but the values determined for the composites are slightly lower (Table 1). The incorporation of particles to copper decreases the copper metallic matrix exposed area, which should lead to a decrease in corrosion current density. On the other hand, the incorporation of particles leads to a decrease of copper grain size, which should lead to a decrease in corrosion resistance [28]. Thus, the slightly higher resistance of the composite coatings when compared to pure copper layers (for a given deposition current density) suggests that the effect of reduction in metallic exposed area on corrosion resistance of composites is predominant.

Table 1 Corrosion potential and corrosion current density of pure copper and Cu–Si_3N_4 composite coatings (obtained using 10 and 30 mA cm^{-2}) in 3.5% NaCl at room temperature

	Cu 10	Cu 30	Cu–Si_3N_4 10	Cu–Si_3N_4 30
E_{corr}/V/SCE	−0.235	−0.233	−0.234	−0.237
i_{corr}/μA cm^{-2}	10.5	12.2	6.9	9.6

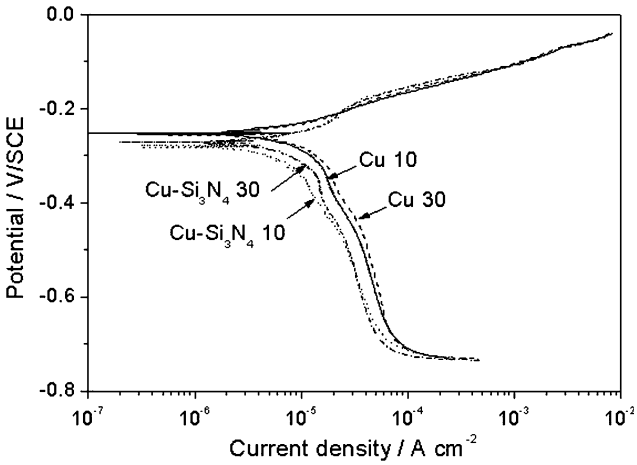

Fig. 10 Polarization curves of pure copper and Cu–Si_3N_4 composite coatings obtained using 10 and 30 mA cm^{-2} current density in 3.5% NaCl solution (for composites 40 g L^{-1} Si_3N_4 concentration)

It is also observed that for both materials, higher corrosion current density was measured for the coatings obtained using 30 mA cm^{-2} deposition current density. This can be attributed to the increase of copper grain boundaries since the increase in deposition current density was shown to reduce the copper grain size for both pure copper and composite coatings. The corrosion resistance of electrodeposits usually decreases as the grain size decreases [28].

4 Conclusions

Smooth Cu–Si_3N_4 composite electrocoatings with uniform particle distribution were obtained on carbon steel by electrolysis of acid sulfate bath containing suspended Si_3N_4 particles.

The incorporation of Si_3N_4 particles to copper did not influence the orientation of copper matrix grains but decreased the copper grain size. Both pure copper and Cu–Si_3N_4 composite electrocoatings showed a preferential growth of copper grains in the [110] direction for 10 and 20 mA cm^{-2} and randomly oriented copper grains for 30 and 40 mA cm^{-2}.

The incorporated particle volume fraction was not influenced by the current density but an increase in particle concentration in the bath from 20 to 40 g L^{-1} led to a decrease in the incorporated particle volume fraction.

The microhardness of the composite coatings was higher than that of pure copper due to dispersion-strengthening

and copper matrix grain refining and increased with the increase of incorporated Si_3N_4 particle content.

The microhardness of both pure copper and composite coatings increased with an increase in cathodic current density due to copper matrix refining.

The composite coatings are slightly more corrosion resistant than pure copper deposits in 3.5% NaCl solutions.

Acknowledgments J.C.P. de Santana and A. Robin acknowledge CNPq (National Council for Development and Research - Brazil) for scholarship and financial support, respectively.

References

1. Hovestad A, Janssen LJJ (1995) J Appl Electrochem 25:519
2. Musiani M (2000) Electrochim Acta 45:3397
3. Celis JP, Roos JR (1977) J Electrochem Soc 124:1508
4. Buelens C, Celis JP, Roos JR (1983) J Appl Electrochem 13:541
5. Hayashi H, Izumi S, Tari I (1993) J Electrochem Soc 140:362
6. Stankovic VD, Gojo M (1996) Surf Coat Tech 81:225
7. Wang YL, Wan YZ, Zhao ShM et al (1998) Surf Coat Technol 106:162
8. Gan YX, Wei CS, Lam M et al (2007) J Mater Sci 42:5256
9. Abdullin IA, Saifullin RS (1997) Prot Met 33:196
10. Medeliene V, Juskenas R, Kurtinaitiene M et al (2004) Pol J Chem 78:1305
11. Benea L, Mitoseriu O, Galland J et al (2000) Mater Corros 51:491
12. Medeliene V, Kurtinaitiene M, Bikulcius G et al (2006) Surf Coat Technol 200:6123
13. Jin ZJ, Zhang M, Guo DM et al (2005) Key Eng Mater 291–292:537
14. Guo DM, Zhang M, Jin ZJ et al (2006) J Mater Sci Technol 22:514
15. Tang JG, Hu K, Fu SH et al (1998) J Appl Polym Sci 69:1159
16. Arai S, Endo M (2005) Electrochem Commun 7:19
17. Zhu LQ, Zhang W, Liu F et al (2004) J Mater Sci 39:495
18. Bund A, Thiemig D (2007) J Appl Electrochem 37:345
19. Aperador Chaparro WA, Lopez EV (2007) Rev Mater 12:583
20. Medeliene V, Kosenko A (2008) Mater Sci 14:29
21. Data Book JCPDS International Centre for Diffraction Data (1978) Selected powder diffraction data—metals and alloys. JCPDS, Swarthmore
22. Stroumbouli M, Gyftou P, Pavlatou EA et al (2005) Surf Coat Technol 195:325
23. Robin A, Fratari RQ (2007) J Appl Electrochem 37:805
24. Zhu J, Liu L, Hu G et al (2004) Mater Lett 58:1634
25. Safranek WH (1974) The properties of electrodeposited metals and alloys. Elsevier, Amsterdam
26. Garcia I, Fransaer J, Celis JP (2001) Surf Coat Technol 148:171
27. Otmacic H, Stupnisek-Lisac E (2003) Electrochim Acta 48:985
28. Dini JW (1993) Electrodeposition: the materials science of coatings and substrates. Noyes Publications, New Jersey